2Pb5-3

Acoustic characterization of lipid bubbles with different shell property

膜物性が異なるリピッドバブルの音響特性評価

Chiaki Kaneko[1†], Yiting Zhang[2], Taro Toyota[2], Hideki Hayashi[3], Shinnosuke Hirata[3], Tadashi Yamaguchi[3], and Kenji Yoshida[3]([1]Grad. School Sci. Eng., Chiba Univ.; [2] Grad. School of Arts and Sci., The Univ. of Tokyo; [3] Center for Frontier Medical Engineering, Chiba Univ.)

金兒 千晶[1†], 章 逸汀[2], 豊田 太郎[2], 林 秀樹[3], 平田 慎之介[3], 山口 匡[3], 吉田 憲司[3*]

([1] 千葉大院 融合理工, [2] 東京大院 総合文化, [3] 千葉大 CFME)

1. Introduction

Near-infrared (NIR) fluorescence imaging has been used to visualize lymph channels and lymph nodes in clinical for the last decade. It has a disadvantage of penetration depth despite superior immediacy, resulting in difficulty visualizing tissue deeper than typically 20 mm. Since ultrasound imaging with better penetration depth and resolution can compensate, we have proposed a dual imaging method with ultrasound and NIR fluorescence imaging. Previously, we fabricated multi-functional particles based on microbubbles (MBs) for dual imaging. The prototype MBs was covered with phospholipid shell incorporating indocyanine green (ICG) derivatives as a contrast agent for NIR fluorescence imaging. It was found that fluorescence intensity, acoustic scattering and attenuation, and the lifetime of the prototype were significantly affected by the lipid composition. However, there are few effects of incorporating ICG derivatives on the performances[1]. Assuming that the state of the phospholipid shell strongly affects the performances, we used three phospholipids with different phase transition temperatures as the main components of the phospholipid shell. This report examined how the membrane permeation resistance and acoustic attenuation depend on the lipid composition.

2. Materials and methods

2.1 Preparation of microbubbles

The contrast agent is composed of a phospholipid membrane and an internal gas. Three types of phospholipids with different phase transition temperatures (T_c), DSPC (1,2-distearoyl-sn-glycero-3-phosphocholine) (T_c = 58°C), DPPC (1,2-palmitoyl-2-oleoyl-sn-glycero-3-phosphocholine) (T_c = 41°C), and POPC (1,2-dipalmitoyl- sn-glycero-3-phosphorylcholine) (T_c = -3°C). DSPC and DPPC were assumed to be in the gel phase at room temperature while POPC was assumed to be in the liquid crystalline phase.

Freeze-ground 2.9×10^{-5} mol phospholipids (DSPC: 22.9 mg, DPPC: 21.3 mg, POPC: 22.1 mg) and 10 mg of PEG-modified phospholipid (DSPE-PEG2000) were mixed in 10 mL of phosphate-buffered saline. The phospholipid dispersion was manually stirred with air or C_6F_{14} gas at a volume ratio of 2:1. Then, it was sonicated with an ultrasonic homogenizer to produce a bubble suspension. Air was used as the internal gas when evaluating the membrane permeation resistance, and C_6F_{14} gas was used when evaluating the attenuation coefficient.

2.2 Analysis of membrane permeation resistance

The system for evaluating the membrane permeation resistance was referred to Ref.1. A thin glass was placed in an acrylic container filled with degassed water. The water temperature and dissolved oxygen concentration were adjusted to 23-25°C and 40-50%, respectively. Bubble suspension was injected under the glass. The bubbles fixed on the glass surface were observed by an optical microscope, and the temporal variations of their radii were evaluated based on the image analysis.

The dissolution model of microbubbles with a shell layer[2] is expressed as

$$-\frac{dR}{dt}=\frac{H}{\frac{R}{D_w}+R_{shell}}\left(\frac{\left(1+\frac{2\sigma}{3P_\alpha R}\right)-f}{1+\frac{4\sigma}{3P_\alpha R}}\right), \qquad (1)$$

where t is the elapsed time, H is the Ostwald coefficient, R is the bubble radius, D_w is the diffusivity of air in the surrounding medium, R_{shell} is the mass transfer resistance of the shell layer, P_a is the ambient pressure, σ is the surface tension of the bubble-water interface, and f is the ratio of the actual partial summer of the diffusing species in the surrounding medium to that at saturation. To estimate R_{shell}, the theoretical calculation of the radius-time (R-t) curve was fitted to the experimental one by using the model.

2.3 Analysis of attenuation coefficient

The system for evaluating the attenuation coefficient in MBs suspension was referred to Ref.1.

†c_kaneko@chiba-u.jp, *kenyoshi1980@chiba-u.jp

A thick acrylic plate was placed as a reflector in an acrylic container filled with ultrapure water. Ultrasound with a center frequency of 10 MHz was emitted from a planar transducer fixed at a position 10 mm above the reflector. The power spectrum of the reflected signal was obtained using a Fourier transform. The reference signal in the absence of MBs was measured preliminarily, and the corresponding power spectrum was also obtained similarly. The attenuation coefficient was calculated using the following equation.

$$\alpha = -8.686 \frac{1}{4d} \ln \frac{P_M}{P_{ref}} \qquad (2)$$

P_{ref} is the power spectrum of the reference signal, P_M is the power spectrum of the reflected signal in the presence of MBs, and d is the distance between the transducer and the reflector.

The distribution of bubble radius was measured using an optical microscope before attenuation evaluation. The radii (mean ± standard deviation) were 1.06 ± 0.44 μm for DSPC MBs, 1.11 ± 0.42 μm for DPPC MBs, and 1.76 ± 0.81 μm for POPC MBs.

3. Results and discussions

Figure 1 shows the membrane permeation resistance for each lipid shell coating MBs. It was found that the DSPC shell had a resistance higher than approximately two times DPPC shell and three times POPC shell. Considering that the phase transition temperatures of DSPC and DPPC were higher than that of degassed water surrounding MBs, DSPC and DPPC shells might keep the gel phase in our experiments. On the other hand, the POPC shell was in the liquid crystal phase, thereby leading to low resistance[2]. Assuming this hypothesis, we will examine the quantitative relationship between the membrane permeation resistance and the phase transition temperature in the future.

Figure 2 shows the attenuation coefficients of DSPC, DPPC, and POPC MBs. The peak frequency of attenuation was found to be around 7-8 MHz in the case of DSPC MBs and 6-7 MHz in the case of DPPC MBs. In contrast, there was no peak in POPC MBs. The decrease with increasing ultrasound frequency suggested that the peak lay in the lower frequency range.

Based on numerous previous studies, we can consider that the peak frequency of the attenuation coefficient is approximately equal to the resonance frequency of MBs. Assuming that the initial radius of a free bubble without shell was 1.1 μm and 1.8 μm, which are the mean radius of DSPC and DPPC MBs in this experiment, the resonant frequency of the free bubble ranged in 4.2 MHz and 2.3 MHz, respectively. Since the peak frequency should increase with increasing the dilatational elasticity of the lipid shell, the DSPC and DPPC MBs coated with the shell of the gel phase should have a higher peak frequency than the free bubble. The peak frequencies of 7-8 MHz in DSPC MBs and 6-7 MHz in DPPC MBs qualitatively agreed with this hypothesis. On the other hand, for POPC coated with liquid crystal phase, the peak frequency lower than 2 MHz suggested that the shell was almost not elastic. In our study, it is essential to compare the dilatational elasticity and viscosity of MBs. We are currently trying to estimate those parameters in various lipids, including DSPC, DPPC, and POPC.

4. Conclusions

We reported the membrane permeation resistance and acoustic attenuation coefficient of three different MBs with DSPC, DPPC, and POPC shells, focusing on the phase transition temperatures. It was suggested that the membrane permeation and the acoustic attenuation of DSPC and DPPC MBs significantly differed from those of POPC MBs, resulting from the difference in the state of the membrane.

Acknowledgment

This work was partly supported by JSPS Grant-in-Aid for Scientific Research 19H04436, 17K11529, and Institute for Global Prominent Research at Chiba University.

References

1. K. Yoshida et al., Jpn. J. Appl. Phys. **60** (2021) SDDE10.
2. M. A. Borden and M. L. Longo, Langmuir 18, 9225 (2002).

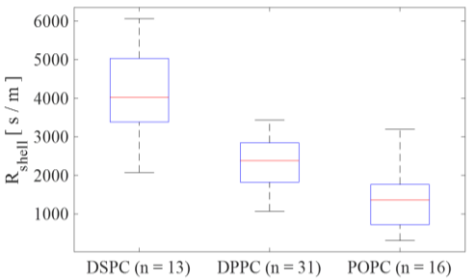

Fig.1 Membrane permeation resistances

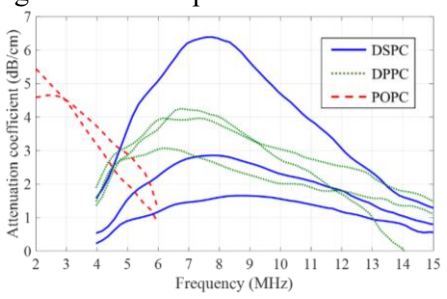

Fig.2 Attenuation coefficients